CHAPTER 15

INVESTIGATING LAND, OCEAN, AND ATMOSPHERE WITH MULTISPECTRAL MEASUREMENTS

15.1 Using Manatee

The MODIS Analysis Toolkit (manatee) has been developed using MATLAB. This chapter will describe some procedures for displaying the MODIS multispectral data using manatee. It should be noted that other versions that do not rely on MATLAB are being investigated. A summary of the manatee commands follows.

Select menu:

- ***Projection*** allows you to put the data in a given projection
- ***Line*** allows you to draw a line on the image (point to the start point, left click with the mouse, point to the end line, and left click with the mouse); this function opens a new window (***Selected Line and Cross Section Plot***) that allows you to plot multiple cross sections along the selected line (use the ***Cross-Section Plot*** command from the new window menu bar)
- ***Region*** allows you to select a region (rectangle) on the image (point to the upper left corner, left click with the mouse, point to the lower right corner, and left click with the mouse).

Plot menu (this is activated only when a line or a region has been selected):

- ***Animate*** makes movies (animations that show different spectral channels)
- ***ScatterPlot*** allows you to linearly combine channels for X and Y axes and to make scatter plots of the selected combinations. Once the ***ScatterPlot*** entry has been selected a new window ***Select Region and Scatter Plot*** pops up. After the channel combinations have been selected and mapped to the X and Y axis, the ***Scatter Plot*** command (on the new window) displays the scatter plot of the selected combinations and activates the ***Subregion*** and ***Get Points*** commands.
- ***Subregion*** allows you to select all the pixels in a rectangle on the image and to identify the locations of these pixels in the scatter plot (move cursor in the image to location of upper left corner of the box then depress the left mouse key and move to the lower right corner of the box and then release the left mouse key)
- ***Get Points*** allows you to select points in the scatter plot image and to identify their spatial Position in the image granule (move cursor in scatter plot to location of upper left corner of the box then depress the left mouse key and move to the lower right corner of the box and then release the left mouse key).
- ***RGB*** combines 3 bands to form an RGB image (this is activated only when a region is selected)
- ***Level 2 Products*** shows products (MODIS cloud mask, Total Precipitable Water, etc) as available

Variables menu:

- ***Radiance/Reflectance*** allows you to select display of radiances or reflectances in the main window;
- ***Radiance/Temperature*** allows selection of radiances or brightness temperatures in the main window.

Settings menu:

- ***Contrast*** allows you to change the extremes of the color scale;
- ***Flip*** allows you to flip the granule up/down or left/right.

Data Output menu: allows the user to output selected variables in different format.

Two points to pay attention to when using manatee. (1) Whenever possible use the ***Close*** command to close different windows, do not exit by killing the window. (2) Most of the windows can be saved in graphical formats by using the ***Edit*** and ***Copy Figure*** commands; the copied figure can then be pasted into a word or power point document.

15.2 Exploring the MODIS spectral bands

The Moderate Resolution Imaging Spectroradiometer (MODIS) on board the Terra and Aqua spacecraft measures radiances in 36 spectral bands between 0.645 and 14.235 μm (King et al. 1992). Table 15.1 lists the MODIS spectral channels and their primary application. Figure 15.1 shows the spectral bands superimposed on the earth reflection and emission spectra. These are repeated from Chapter 13 for convenience. A summary of the some of the relevant spectral properties is presented in Figure 15.2.

Using manatee, analyze the remote sensed measurements in a granule of MODIS data. Proceed with the following steps. Start up MATLAB and use the "**...**" command to point MATLAB at the manatee directory. In response to the "**>>**" prompt, type in "***manatee***". Once the MODIS Display is engaged, use the ***Load Data*** command on the top of the display to load an image file from the data base. Select a granule in hdf format (for example the cloud scene over Italy on 29 May 2001 stored in MOD021KM.A2001149.1030.003.2001154234131.hdf). Select the longwave infrared window (LIRW) ***Band number*** (Band 31), and display it as radiance (rather than brightness temperatures) using ***Radiance*** (under the ***Variables*** tool). See Figure 15.3.

Try out different ***Contrast*** (under the ***Select*** tool), and ***Select projection*** (under the ***Select*** tool). Get familiar with the command menu by trying out different bands and combinations of contrast and projection. Figure 15.4 shows a mercator projection of the MODIS scene covering southern Europe, northern Africa, and the Mediterranean Sea in between.

15.2.1 Use ***Select Region*** (under the ***Select*** tool) to select a region within the image. To do this move cursor to location of upper left corner of the box then depress the left mouse key and move to the lower right corner of the box and then release the left mouse key (see Figure 15.5 for an example covering the Alps, northern Italy, and the Adriatic Sea). It is interesting to ***Animate*** (under the ***Plot*** tool) some of the spectral bands; and to notice how the cloud, atmosphere, and surface features appear in each band (not shown).

15.2.2 Use ***Scatter Plot*** (under the ***Plot*** tool) to investigate the temperatures in the Selected Region display. Plot a scatter plot of LIRW (Band 31) and SIRW (Band 21) brightness temperatures (BT). Note that the BT(SIRW) are typically greater than the BT(LIRW) because the atmosphere is more transparent in the SIRW and there are some contributions from reflected solar radiation in the SIRW that are not present in the LIRW. As you move the cursor over the image BT(LIRW) values are indicated bottom right below the image. Note that the maximum BT(LIRW) occur along the coast the northern Africa and the minimum BT(LIRW) appear in the high opaque clouds. Engage the ***SubRegion*** command to select a subregion in the image (move cursor in the image to location of upper left corner of the box then depress the left mouse key and move to the lower right corner of the box and then release the left mouse key) and observe where the pixels in the sub-region occur in the scatter plot. Select some cloud and some clear surface. Figure 15.7 reveals that BT(SIRW) values are warmer than BT(LIRW) in cloudy scenes but they are roughly the same over non-vegetated land. Close the Selected Region display (upper right menu command).

15.2.3 Use ***Select Line*** (under the Select tool) to draw a line through the two cloud banks north-east and south-west of Italy (see Figure 15.8). To do this, point to the start point, left click with the mouse, point to the end line, and left click with the mouse. Highlight bands 31 through 36 in the Selected Line and Cross Section Plot display (opened by ***Select Line***). Exercise the ***Cross Section Plot*** command. Note how the band temperatures change from position A to B to C to D on the cross section plot. Note that the band temperatures most alike in the high opaque clouds where the radiances do not transmit through very much of the atmosphere and hence do not encounter very much CO2. In the less opaque clouds (southwest of C) some differences in the band temperatures

are noticeable. The band temperatures are most different in clear skies where transmission through the whole atmosphere must be accomplished by radiation in each spectral band; the differing CO2 sensitivities of the spectral bands cause most of the radiation from each spectral band to emanate from different layers of the atmosphere. At the centre of the CO2 absorption band, radiation from the upper levels of the atmosphere (e.g. radiation from below has already been absorbed by the atmospheric gas) are sensed. From spectral regions away from the centre of the absorption band, radiation from successively lower levels of the atmosphere are sensed. Away from the absorption band, the windows to the bottom of the atmosphere are found. Close this display when you are finished.

15.2.4 Select ***Band number*** 27 (6.7 μm) on the MODIS Display and use ***Variables*** to select ***temperature***. This WV band is used in cloud detection but also to derive upper tropospheric humidity (UTH). Dry slots (connected by the line) are evident in the 6.7 μm (band 27) water vapor sensitive image and upper level opaque clouds are apparent toward the northwest. In addition in the image, detector-to-detector differences show up as striping (and are also very evident in the cross section plot along the indicated line). The striping can be mitigated using the empirical distribution function technique of Weinreb et al (1989). The technique uses a reference detector and makes the distribution function of the other detector match that of the reference detector. This approach maintains radiometric calibration and minimizes the differences between detectors. Close this display when you are finished. The destriping reference is Weinreb, M. P., R. Xie, J. H. Lienesch, and D. S. Crosby, 1989. Destriping GOES Images by matching empirical distribution functions. Remote Sens. Environ, 29, 185-195.

15.2.5 Display ***band number*** 1 (0.65 μm) ***reflectance*** values. ***Select*** a region covering the Alps, northern Italy, and the Adriatic Sea (as selected in Figure 15.5). Upon investigating the radiances emanating from the scene in different wavelengths, use ***Plot/RGB*** to image bands 1 (0.65 μm), 6 (1.64 μm), and 31 (11 μm). Figure 15.11 shows how the low 1.6 μm reflectance in Alpine snow contrasts with high 1.6 μm reflectance in ice clouds helping to distinguish between the two (see Figure 13.5a to help understand this change in reflectance).

15.2.6 Use ***Plot/ScatterPlot*** to combine spectral bands that are useful for characterizing surface and cloud features (hit return after entering each number in the box). The band combination [band 2 (0.86 μm) / band 1 (0. 65 μm)] plotted on the x-axis and band 31 (11 μm) plotted on the y-axis is shown in Figure 15.12. Using the ***Get Points*** function to select points in the scatter plot (move cursor in scatter plot to location of upper left corner of the box then depress the left mouse key and move to the lower right corner of the box and then release the left mouse key) and to map them on the MODIS scene. Figure 15.12 reveals that clouds are found when the band ratio (2/1) is near one and band 31 is cold (green box) and non-vegetated land appears when the band ratio (2/1) is near one and band 31 is hot (brown box). Vegetated land appears when the band ratio is much greater than 1 (blue box). Figure 15.13 shows the snow index [band 1 (0.65 μm) – band 6 (1.6 μm) / band 1 (0.65 μm) + band 6 (1.6 μm)] helping to distinguish snow (near one) from clouds (near zero). Warmer surface temperatures with snow index near one are sometimes outlining ocean features. An image of the snow index as a pseudo-channel is displayed in Figure 15.14; it is generated by using the ***PseudoChannel*** function and selecting the x-axis.

15.3 Detecting Clouds

15.3.1 Cloud detection can be refined using spectral band combinations that include 0.65, 0.85, 1.38, 1.6, 8.6, and 11 μm. Multispectral investigation of a scene can separate cloud and clear scenes into various classes. Cloud and snow appear very similar in a 0.65 μm image, but dissimilar in a 1.6 μm image (Figure 15.2 indicates that snow reflects less at 1.6 than 0.65 μm). For 8.6 μm ice/water particle absorption is minimal, while atmospheric water vapor absorption is moderate. For 11μm, the opposite is true. Using these two bands in tandem, cloud properties can be distinguished. Large positive values of [BT8.6 - BT11] indicate the presence of cirrus clouds; negative differences indicate low water clouds or clear skies. Cloud boundaries are often evident in local standard deviation of radiances. The 1.38 μm offers another opportunity to detect high thin cirrus; this channel images the upper troposphere and is highly sensitive to the presence of ice crystals.

Focus on the thin cloud region in the northwest corner of the image. Use ***Plot/ScatterPlot*** to view band 31 (11 μm) versus [band 29 (8.6 μm) - band 31 (11 μm)] and with the ***PseudoChannel*** option construct its image in Figure 15.15. The largest positive differences are found in ice clouds and negative differences occur in water clouds. Some of these clouds are not evident in the visible image at 0.65 um (see Figure 15.16). Band 26 (1.38 μm) is sensitive to water and ice reflectances from the upper half of the troposphere; Figure 15.17 reveals the contrails of ice cloud very clearly.

15.3.2 Select a small region within the cloud band northeast of Italy. Plot the brightness temperature differences [band 29 (8.6μm) - band 31 (11μm)] on the x-axis and [band 31 (11μm) - band 32 (12μm)] on the y-axis. Figure 15.18 shows the hook shaped scatter plot resulting from partially clear and cloud contributions to the brightness temperature in each spectral band. The Planck function radiance at shorter wavelengths is dependent on temperature to a higher power than the Planck radiances at longer wavelengths, thus the warmer part of the pixel contributes more to the brightness temperature at shorter wavelengths.

To see this more clearly consider a calculation for broken clouds. Assume Tclr=300 and Tcld=230. Recalling the discussion in Chapter 2 on temperature sensitivity of the Planck function,
$dB/B = \alpha\, dT/T$ where $\alpha \approx c_2\nu/T$ implies that B is proportional to T^{α}. Thus the cold part of pixel has more influence at longer wavelengths (lower wavenumbers).

B12 ≈ = (1-N)*Tclr**4.1+N*Tcld**2.8~(1-N)*300**4.1+N*200**2.8
B11 ≈ = (1-N)*Tclr**4.3+N*Tcld**2.9~(1-N)*300**4.3+N*200**2.9
B8.6 ≈ (1-N)*Tclr**5.6+N*Tcld**3.7~(1-N)*300**5.6+N*200**3.7

≈ 293.5, ≈ 293.8, and BT8.6 ≈
Then when the brightness temperature differences in the scatter plot are considered,

$[BT11(N)-BT12(N)] = [(1-N)*B11(Tclr)+N*B11(Tcld)]^{-1} - [(1-N)*B12(Tclr)+N*B12(Tcld)]^{-1}$
$[BT8.6(N)-BT11(N)] = [(1-N)*B8.6(Tclr)+N*B8.6(Tcld)]^{-1} - [(1-N)*B11(Tclr)+N*B11(Tcld)]^{-1}$

we find that as we move from clear (N=0) to cloudy (N=1) skies they arrange themselves in a hook shape as found in Figure 15.18. The spectral dependence of the cloud emissivity will modify the results of this simple calculation somewhat, but the dominating influence is from the Planck function.

This also demonstrates why cloud edges introduce difficulties to cloud detection techniques that rely on threshold brightness temperature differences to indicate cloud presence. Figure 15.19 shows the cloud mask from the operational algorithm (described in Chapter 6); good skill is evident in distinguishing clear from cloudy skies, except near cloud edges where threshold tests have difficulty.

15.4 Mapping Vegetation

The vegetation index is based on the relatively low leaf and grass reflectance from spectral bands below 0.72 μm and relatively high reflectance from spectral bands above. A pseudo image of normalized vegetation index [band 2 (0.86μm) – band 1 (0.65μm)] / [band 2 (0.86μm) + band 1 (0.65μm)] is displayed in Figure 15.20. Regions with some vegetation are clearly distinguished from those with little. Regions without significant vegetation have indices below 0.3; vegetated regions show indices above 0.6.

15.5 Investigating a Dust Storm

Use ***Load Data*** in the MODIS Display to load MODIS measurements of a dust storm in Iran on 11 June 2001 (MOD021KM.A2001162.0645.003.2001167183512.hdf). Select Region to focus on the dust storm (see Figure 15.21). Figure 15.22 shows the ***ScatterPlot*** of [Band 31 - Band 32] on the x-axis and [Band 29 (8.6μm) minus Band 31 (11 μm)] on the y-axis; the dust storm produces negative temperature differences (between 0 and –2 C) in both window pairs. Comparing Figure 15.22 with a

comparable figure in clouds (Figure 15.18) reveals that clouds produce positive temperature differences (between 0 and 4 C). Discrimination of dust storms and clouds should be possible with these spectral bands. Figure 15.23 shows a pseudo channel plot over the dust storm of [BT(8.6 um) – BT(11um)]; the dust storm produces the least negative values in the scene.

15.6 Investigating a Volcanic Eruption

Use ***Load Data*** in the MODIS Display to load MODIS measurements of a volcanic eruption of Mt Etna on 28 October 2002 (MOD021KM.A2002301.1215.003.2002302200901.hdf). Select Region to focus on the eruption (see Figure 15.24). Figure 15.25 shows the ***ScatterPlot*** of [Band 31 - Band 32] on the y-axis and Band 31 (11 μm) on the x-axis. The volcanic ash produces negative temperature differences (between 0 and –6 C) in the split window; the denser ash produces the larger differences.

15.7 Investigating Coastal Waters (SST and Chlorophyll)

Use ***Load Data*** in the MODIS Display to load MODIS measurements of Western Australia on 19 August 2000 (MOD021KM.A2000232.0300.004.2002365101900.hdf). Focusing on the Shark Bay region, Figure 15.26 shows a pseudo image of the sea surface temperature derived from the split window band 31 (11μm) and band 32 (12μm). It is obvious that the waters within Shark Bay are much cooler than the Leeuwin current waters along the WA coastline. Figure 15.27 shows a scatter plot of band 31 (11μm) on the x-axis and (band 9 (0.44μm) / band 12 (0.57μm) on the y-axis. Band 9 has relatively high and band 12 has relatively low water absorption for chlorophyll; the low ratio values are an indication of chlorophyll concentrations.

15.8 Summary

New multispectral sensors such as MODIS, MERIS, GLI, and MSG are capable of producing a variety of enhanced products that include (a) cloud detection, (b) aerosol concentration and optical properties during the day, (c) cloud optical thickness, thermodynamic phase, and top temperature, (d) vegetation and land surface cover, (f) snow and sea-ice cover, (g) surface temperature, and (h) ocean color. These capabilities will be continued into the future with VIIRS, ABI, MTSAT-R, and others.

Table 15.1: MODIS Channel Number, Wavelength (μm), and Primary Application

Reflective Bands		
1,2	0.645, 0.865	land/cld boundaries
3,4	0.470, 0.555	land/cld properties
5-7	1.24, 1.64, 2.13	land/cld properties
8-10	0.415, 0.443, 0.490	ocean color/chlorophyll
11-13	0.531, 0.565, 0.653	ocean color/chlorophyll
14-16	0.681, 0.75, 0.865	ocean color/chlorophyll
17-19	0.905, 0.936, 0.940	atm water vapor
26	1.375	cirrus clouds
Emissive Bands		
20-23	3.750(2), 3.959, 4.050	sfc/cld temperature
24,25	4.465, 4.515	atm temperature
27,28	6.715, 7.325	water vapor
29	8.55	sfc/cld temperature
30	9.73	ozone
31,32	11.03, 12.02	sfc/cld temperature
33-36	13.335, 13.635, 13.935, 14.235	cld top properties

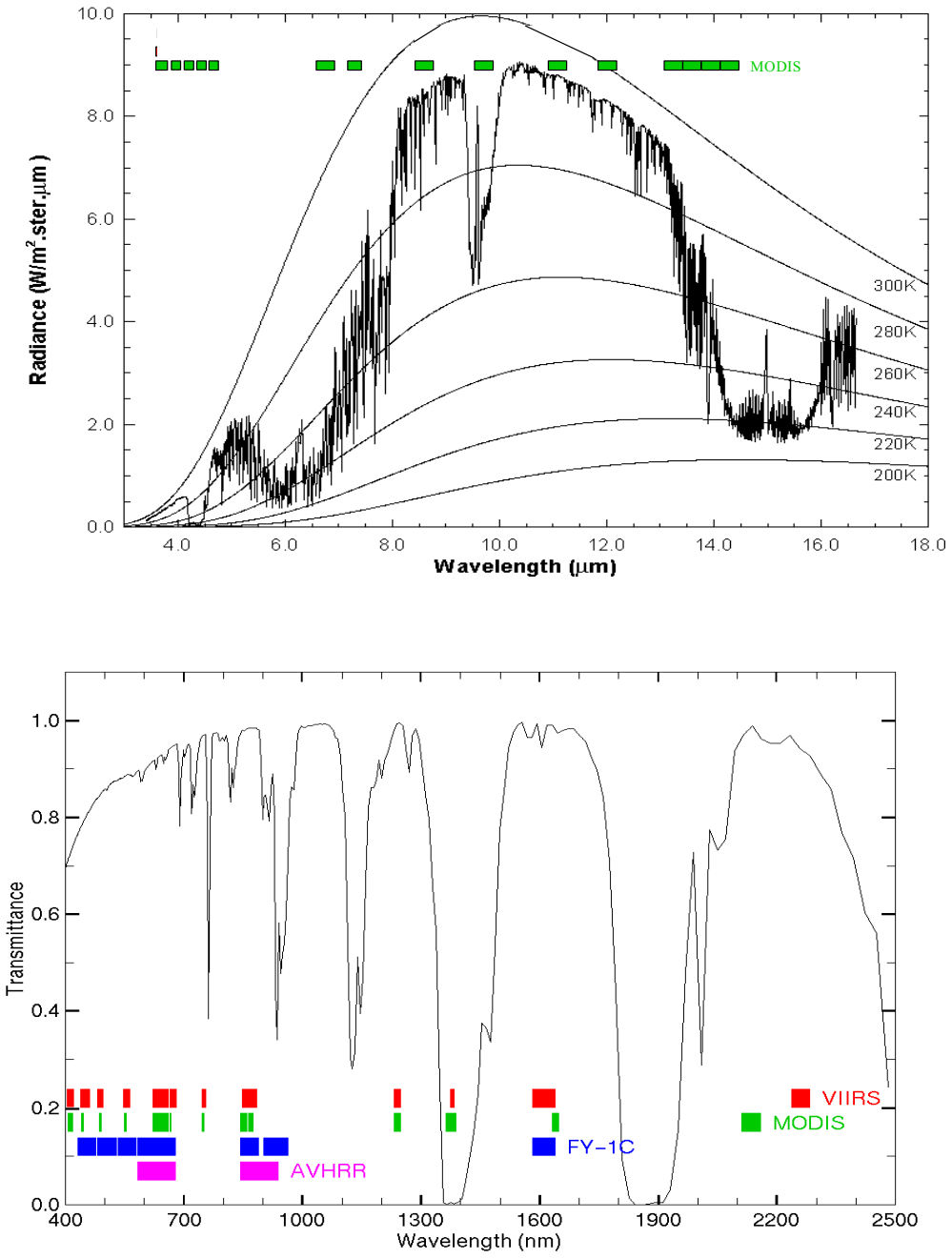

Figure 15.1: MODIS emissive bands superimposed on a high resolution earth atmosphere emission spectra with Planck function curves at various temperatures superimposed (top) and MODIS reflective spectral bands superimposed on the earth reflection spectra (bottom).

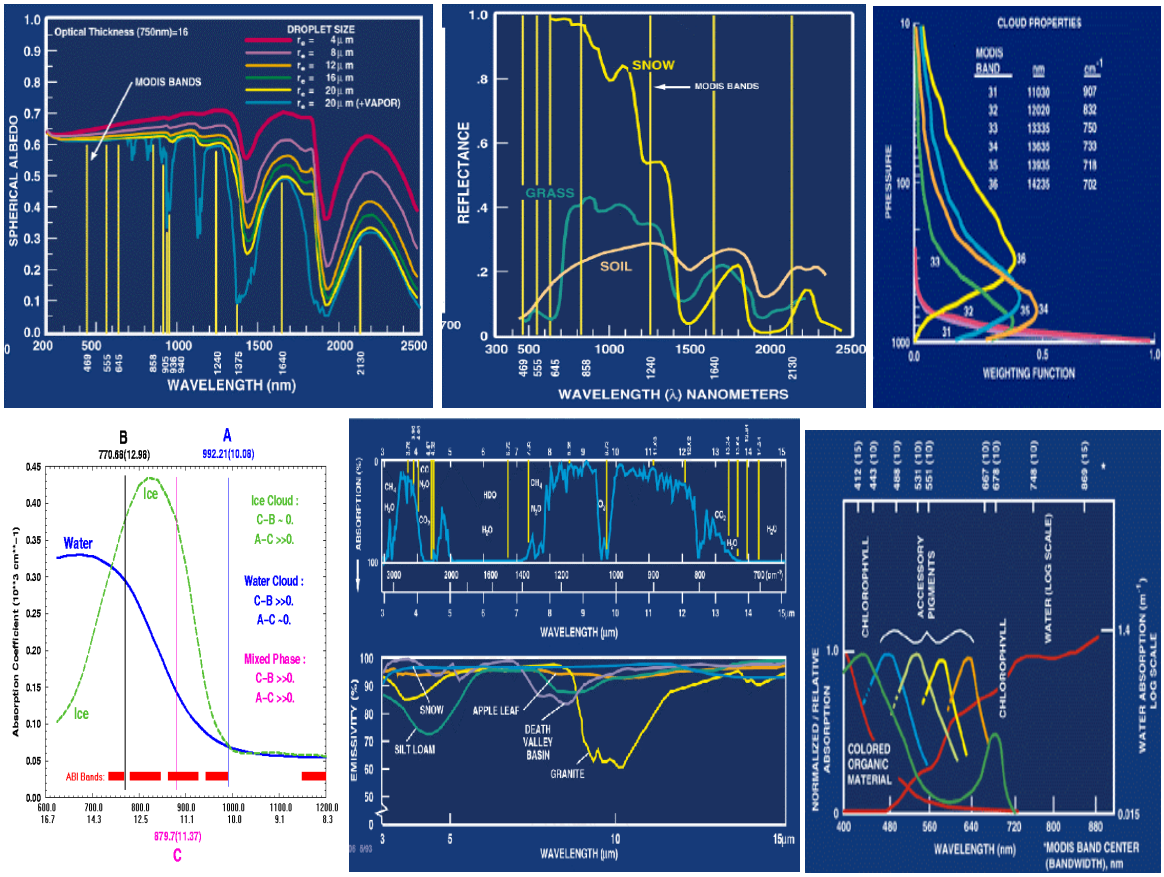

Figure 15.2: Summary of spectral reflectance for various surfaces between 0.3 and 2.5 um (top left and middle), weighting functions for CO2 bands (top right), water and ice cloud absorption in the LIRW region (bottom left) and atmospheric transmission and surface emissivity from 3 to 15 um (bottom center), and water absorption of chlorophyll and accessory pigments from 0.4 to 0.9 um (bottom right).

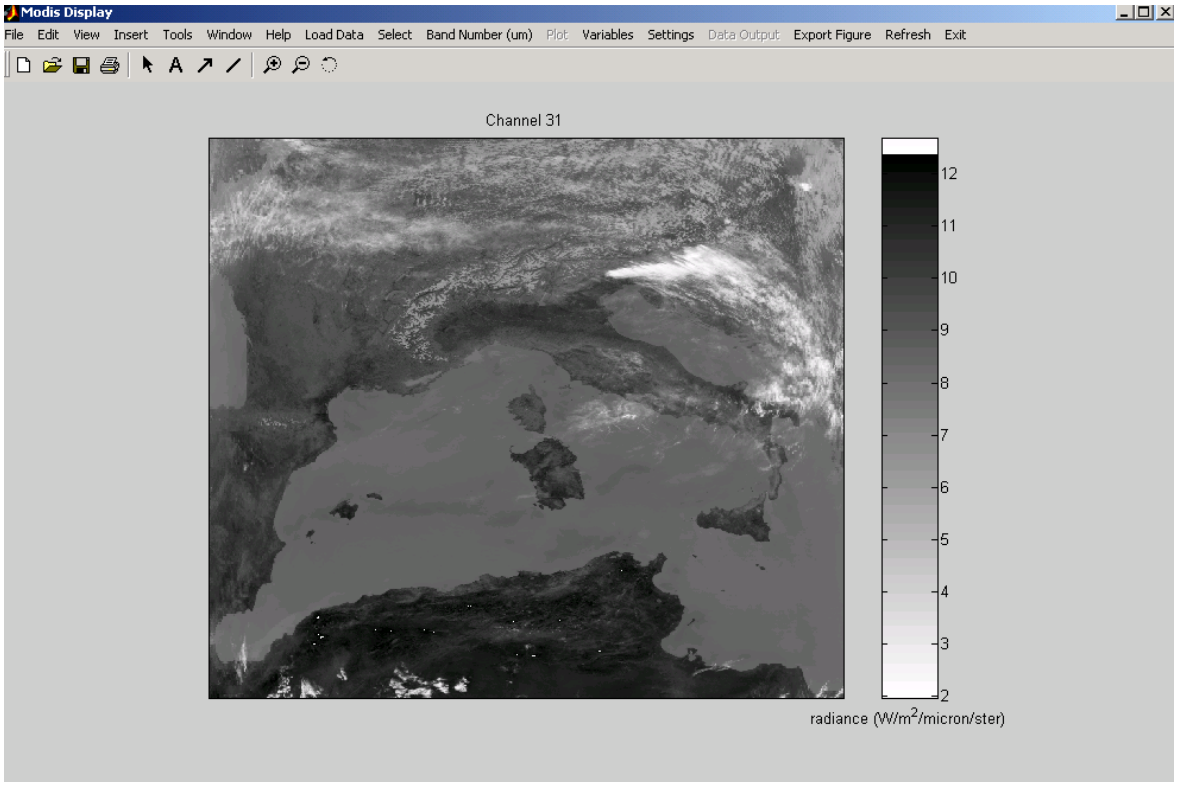

Figure 15.3: MODIS Display (in manatee) of MODIS IRW (Band 31) radiances (W/m2/micron/ster) with the tool bar indicated at the top of the screen.

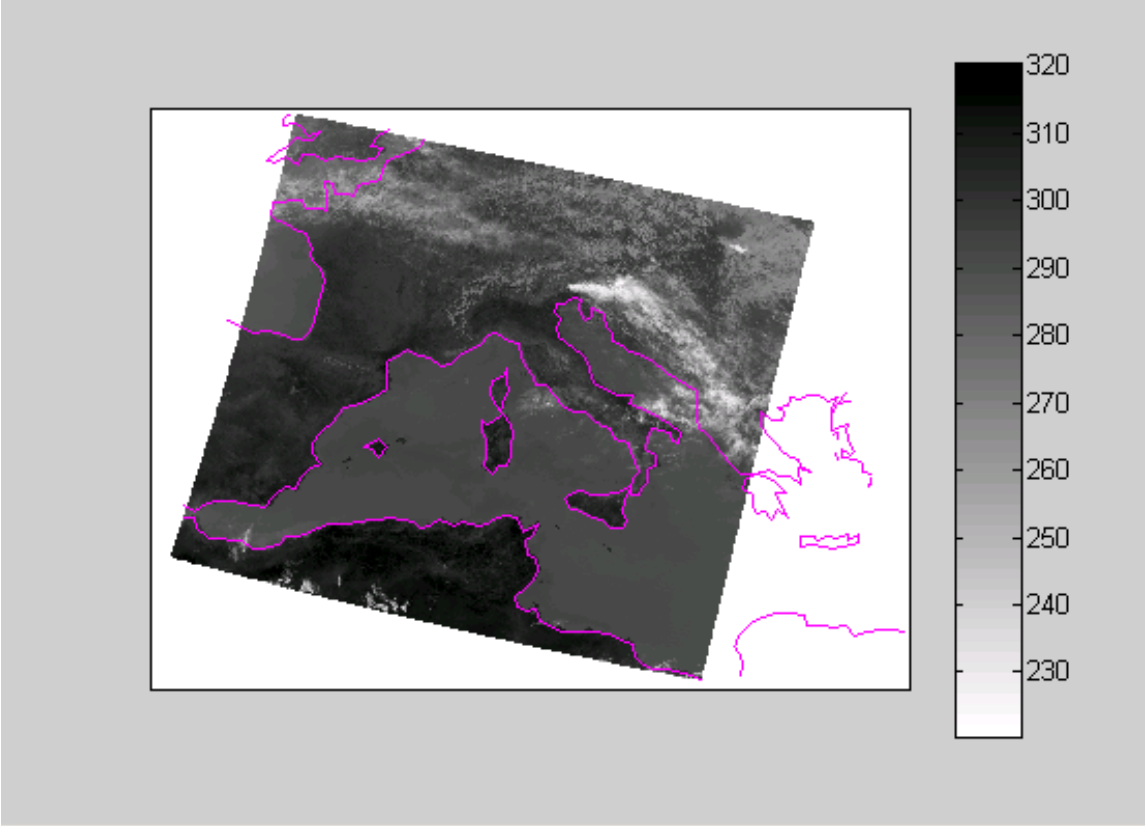

Figure 15.4: MODIS IRW (Band 31) image displayed in a mercator projection indicating coastlines for reference.

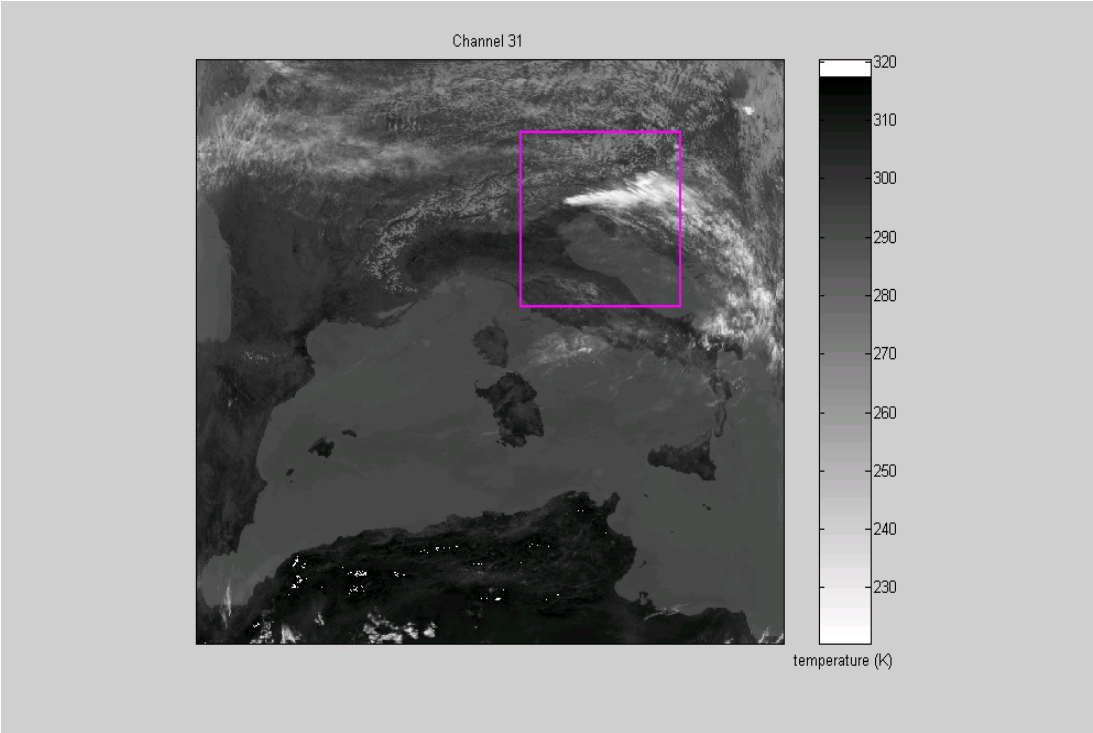

Figure 15.5: Selected region in Alps, northern Italy, and the Adriatic Sea superimposed on the MODIS IRW (Band 31) brightness temperature (BT) image.

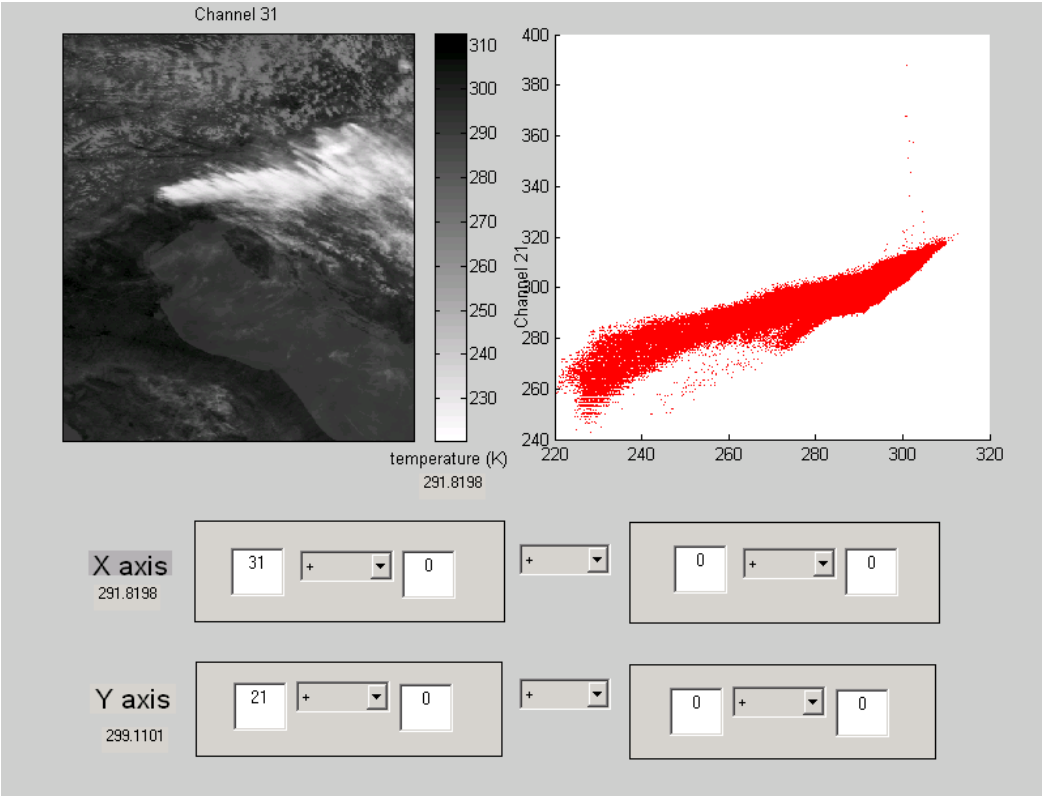

Figure 15.6: Scatter plot of BT(SIRW, Band 21) on the y-axis and BT(LIRW, Band 31) on the x-axis for the selected region in Alps, northern Italy, and the Adriatic Sea.

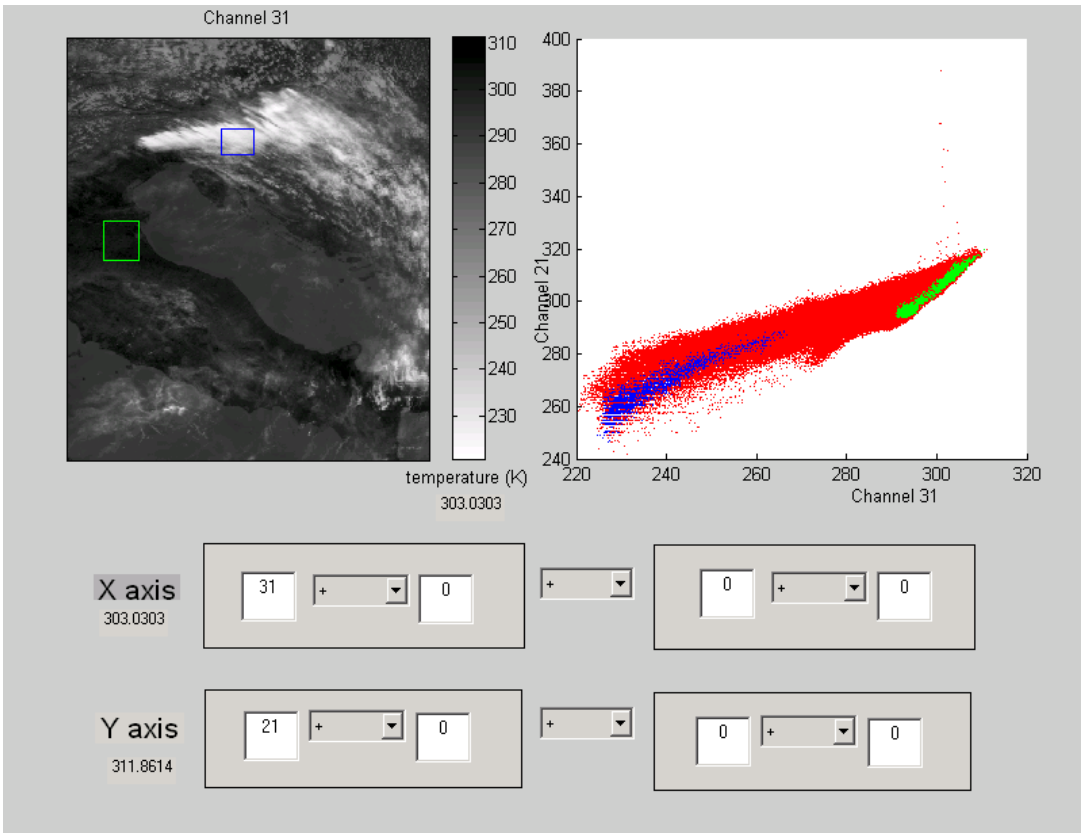

Figure 15.7: Same as Figure 15.4. BT(SIRW) values are warmer than BT(LIRW) in cloudy scenes (blue); they are roughly the same over non-vegetated land (green).

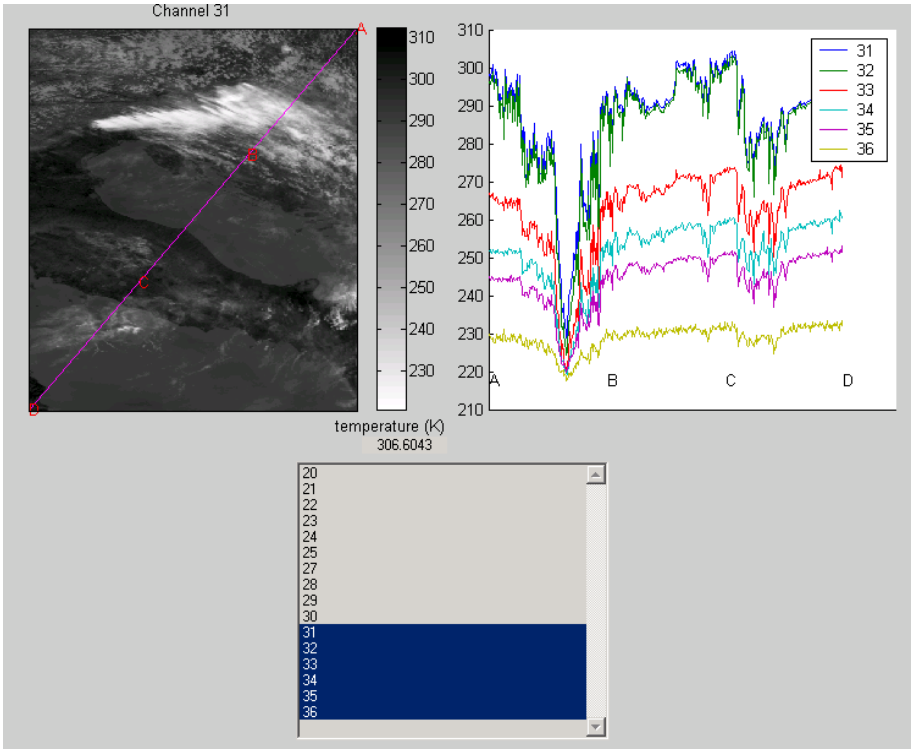

Figure 15.8: Cross-section plot of BT(CO2) for the LIRW and CO2 sensitive bands moving from the northeast to the southwest in the image (from A to B to C to D)

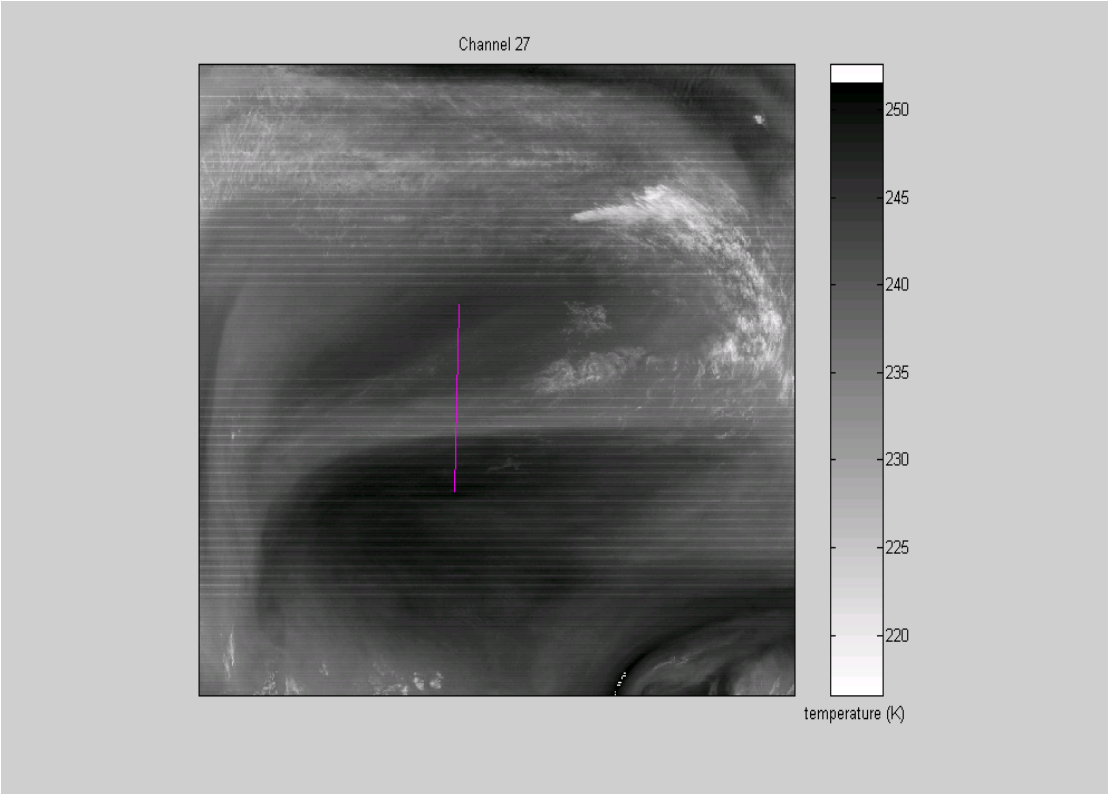

Figure 15.9: Dry slots (connected by the line) in the 6.7 um water vapor sensitive image of band 27. Upper level opaque clouds are apparent in the northwest.

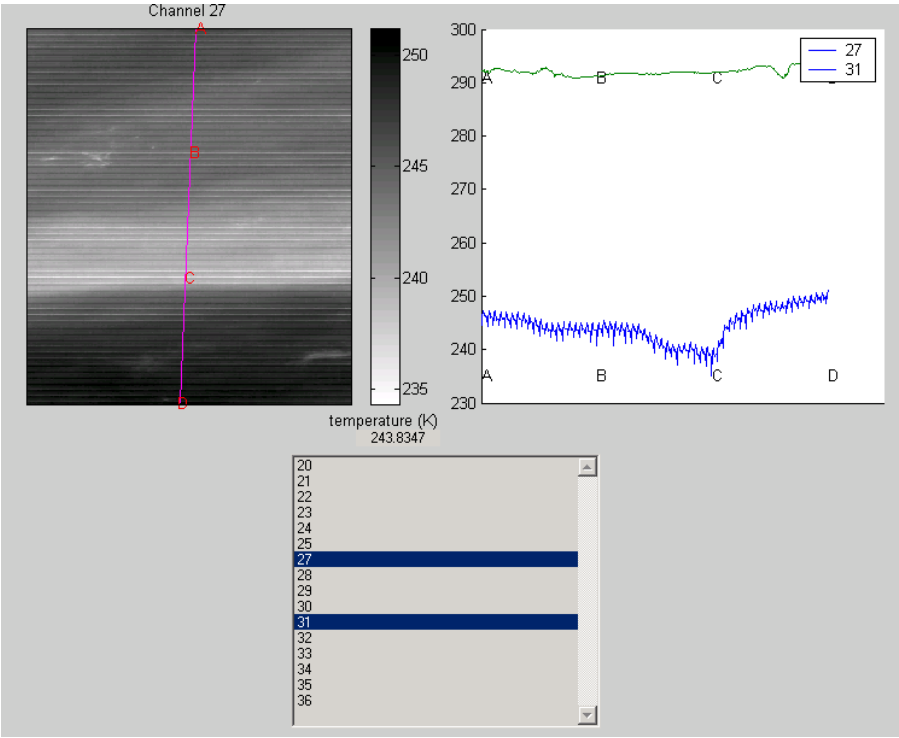

Figure 15.10: Cross-section plot of BT(H2O) for the 6.7 μm (band 27) water vapor sensitive band from north to south from one dry slot to another (from A to B to C to D). The dry slots are about 10 C warmer than the wet slots. BT(LIRW) for the 11 μm (band 31) are also shown and are found to be 40 to 50 C warmer.

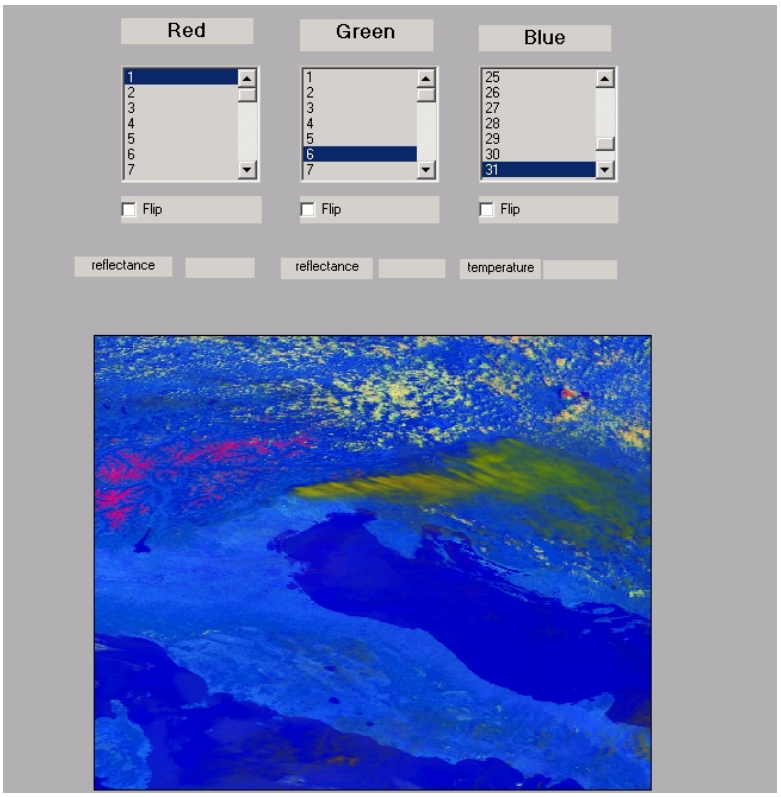

Figure 15.11: RGB plot with 0.65 μm (band 1) displayed as red, 1.6 μm (band 6) displayed as green, and 11 μm (band 31) displayed as blue. Note how the low 1.6 μm reflectance of snow in the Alps contrasts with high ice cloud 1.6 μm reflectance helping to distinguish between the two.

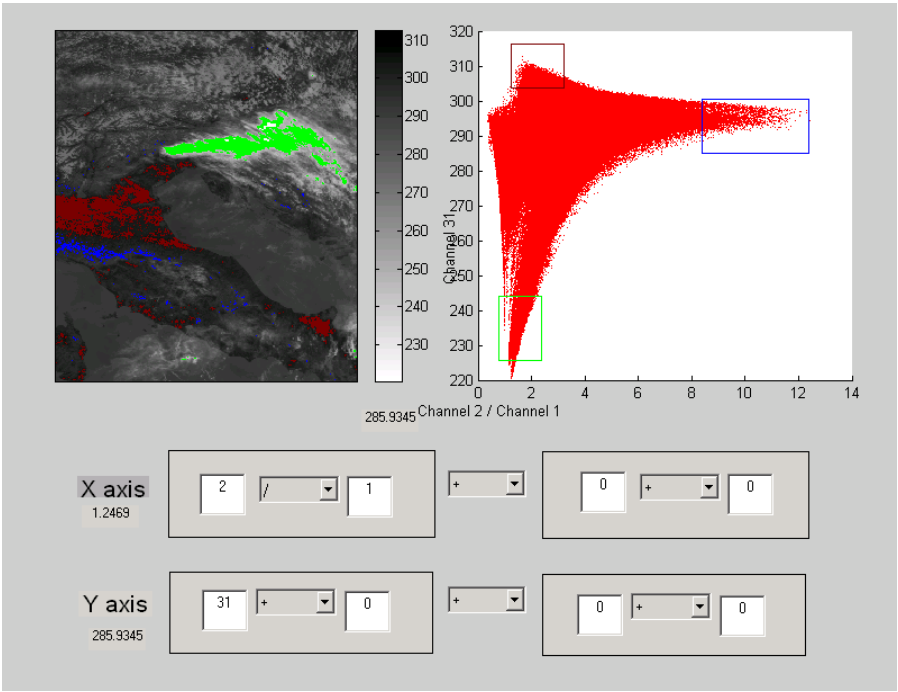

Figure 15.12: Scatter plot of [band 2 (0.86 μm) / band 1 (0. 65 μm)] on the x-axis and band 31 (11 μm) on the y-axis. Clouds are found when the band ratio (2/1) is near one and band 31 is cold (green box), non vegetated land appears when the band ratio (2/1) is near one and band 31 is hot (brown box), and vegetated land appears when the band ratio is much greater than 1 (blue box).

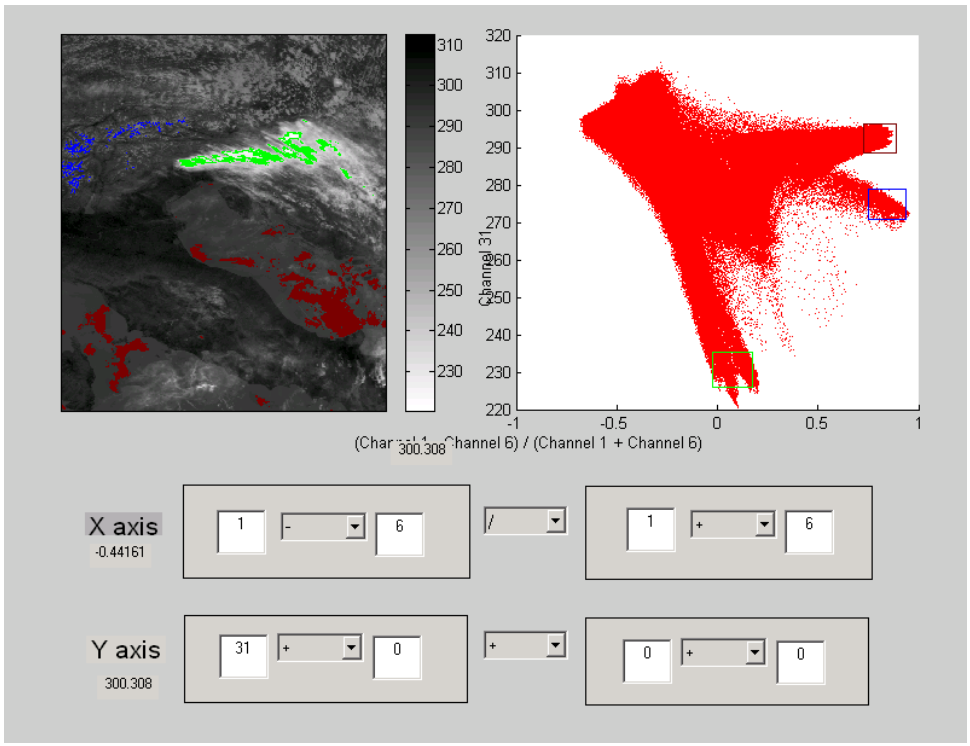

Figure 15.13: Scatter plot of the snow index [band 1 (0.65 μm) – band 6 (1.6 μm) / band 1 (0.65 μm) + band 6 (1.6 μm)] on the x-axis and band 31 (11 μm) on the y-axis band. Snow (index near one in blue) is distinguished from clouds (index near zero in green). Warmer surface temperatures with snow index near one are sometimes outlining ocean features (in brown).

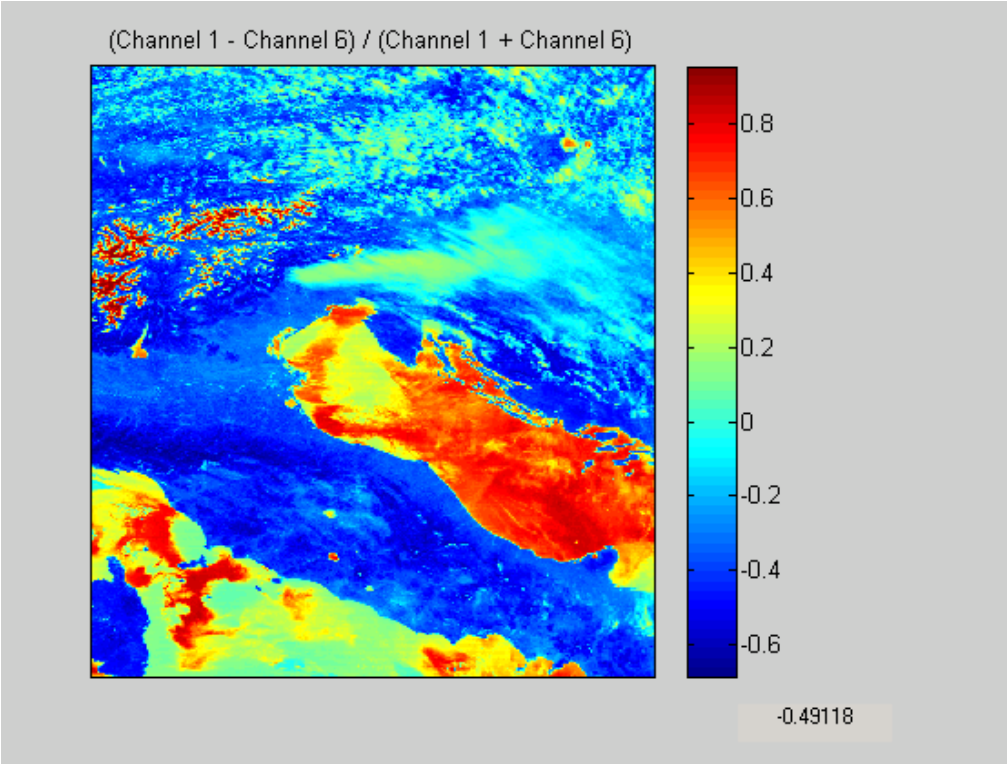

Figure 15.14: Color image of the snow index as a pseudo-channel. High values near one (when reflectivity in 1.6 um is low) indicate snow in the mountains or ocean surfaces with much higher reflectivity at 0.65 um than at 1.6 um.

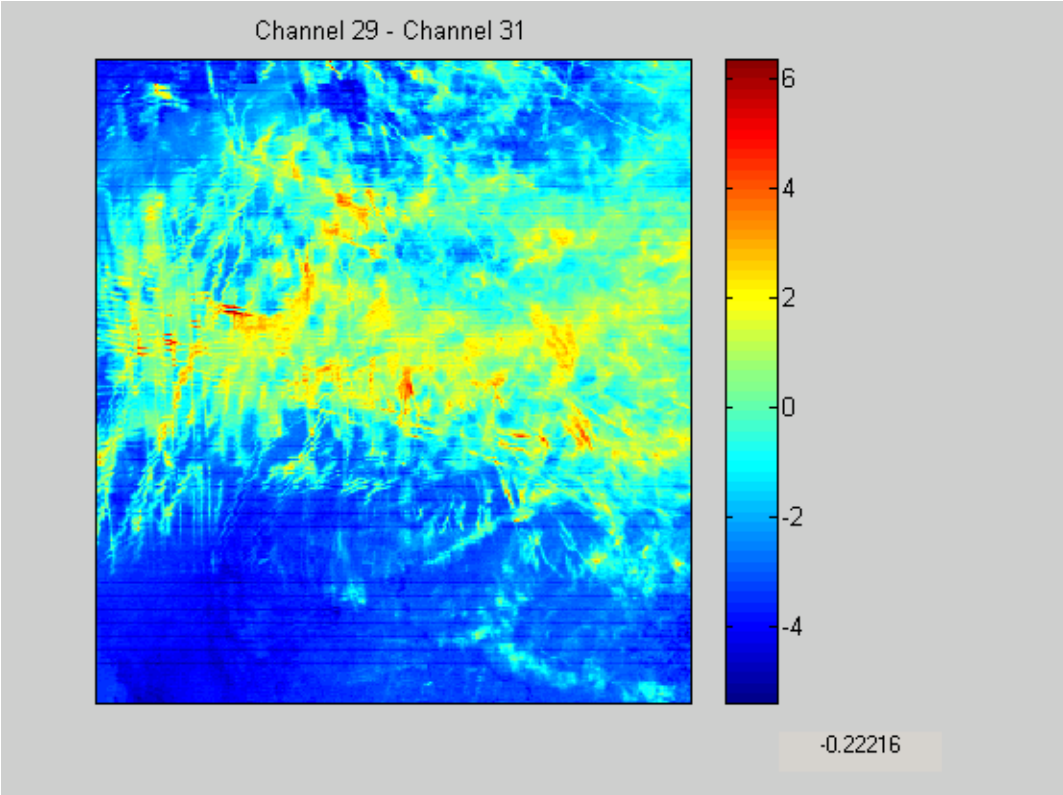

Figure 15.15: Pseudo channel plot on [BT(8.6 um) – BT(11 um)]. Positive values indicate ice clouds. Note straight line clouds produced by aircraft contrails.

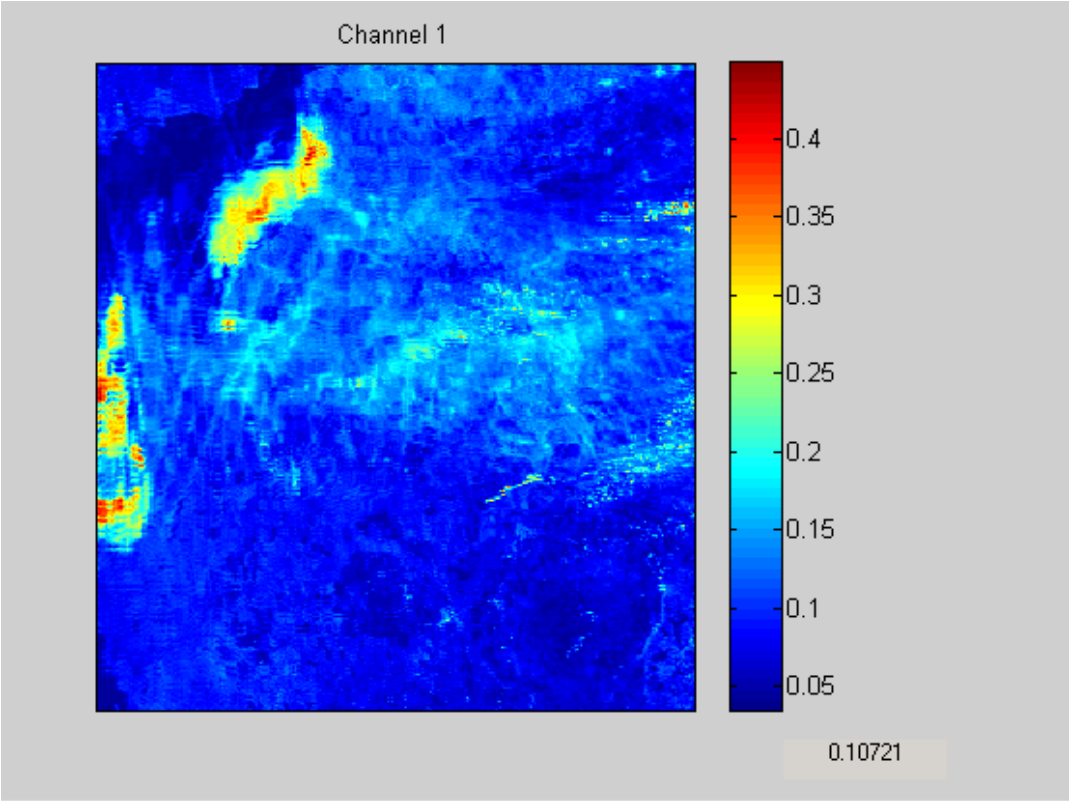

Figure 15.16: Color image of the 0.65 um channel. Note that many of the clouds detected in the infrared 8.6 um – 11 um image (Figure 15.12) are not evident in the visible.

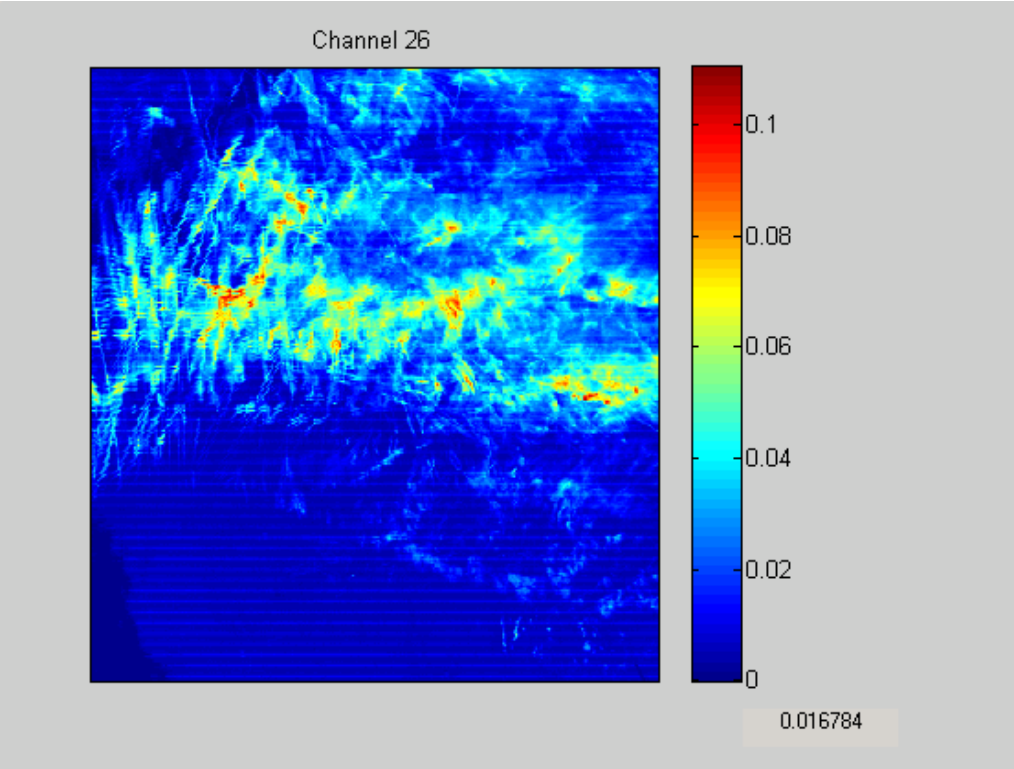

Figure 15.17: Color image of the 1.38 um channel. Note that the ice cloud contrails detected in the infrared 8.6 um – 11 um image (Figure 15.12) are clearly evident in this near infrared channel.

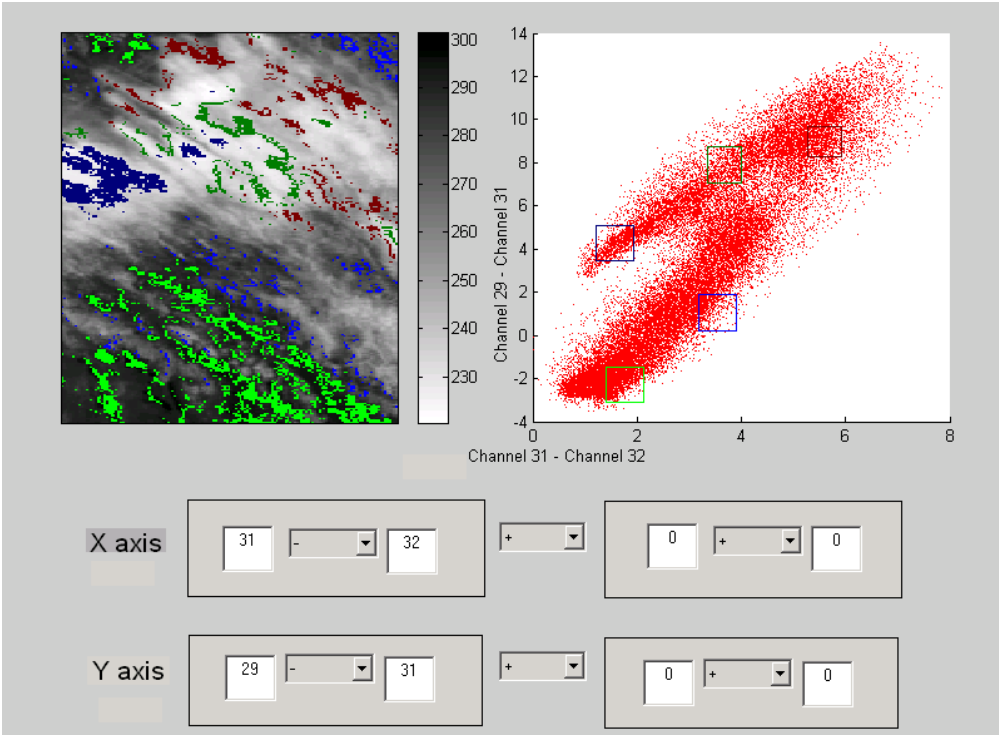

Figure 15.18: Scatter plot of brightness temperature differences [band 29 (8.6μm) - band 31 (11μm)] on the y-axis and [band 31 (11μm) - band 32 (12μm)] on the x-axis. Color boxes in the scatter plot move along the hook shape from mostly clear skies (green), to cloudier skies (light blue, brown, and dark green) to cloudiest skies dark blue).

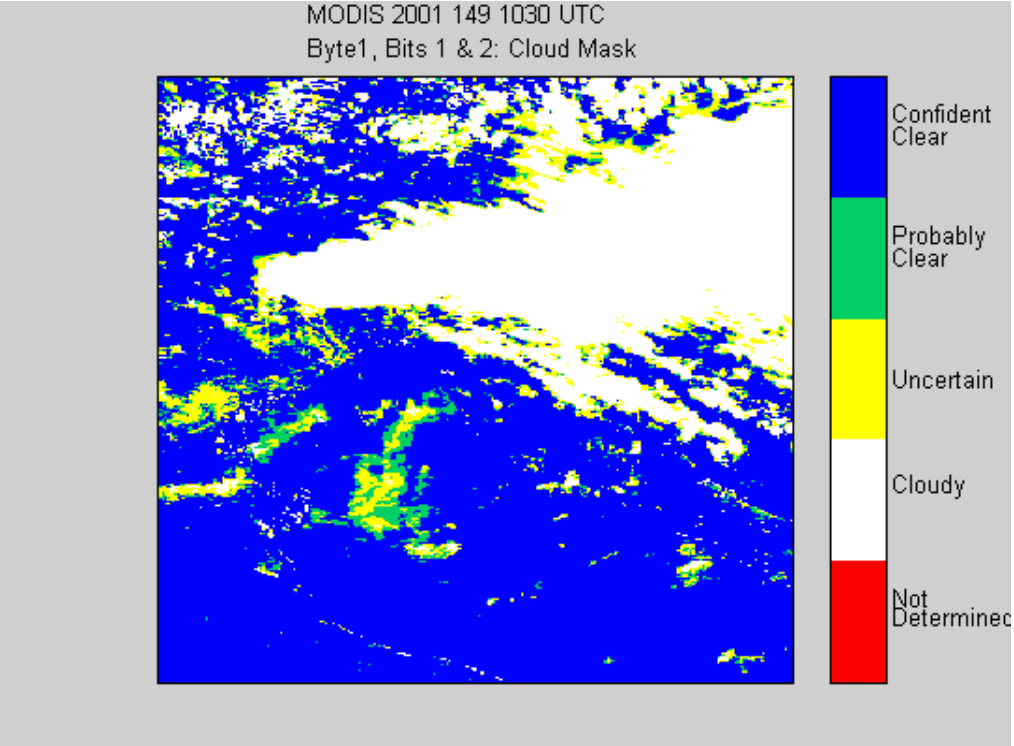

Figure 15.19: Cloud mask from the operational algorithm (described in Chapter 6) showing good skill in distinguishing clear from cloudy skies, except near the cloud edges where threshold techniques have difficulty.

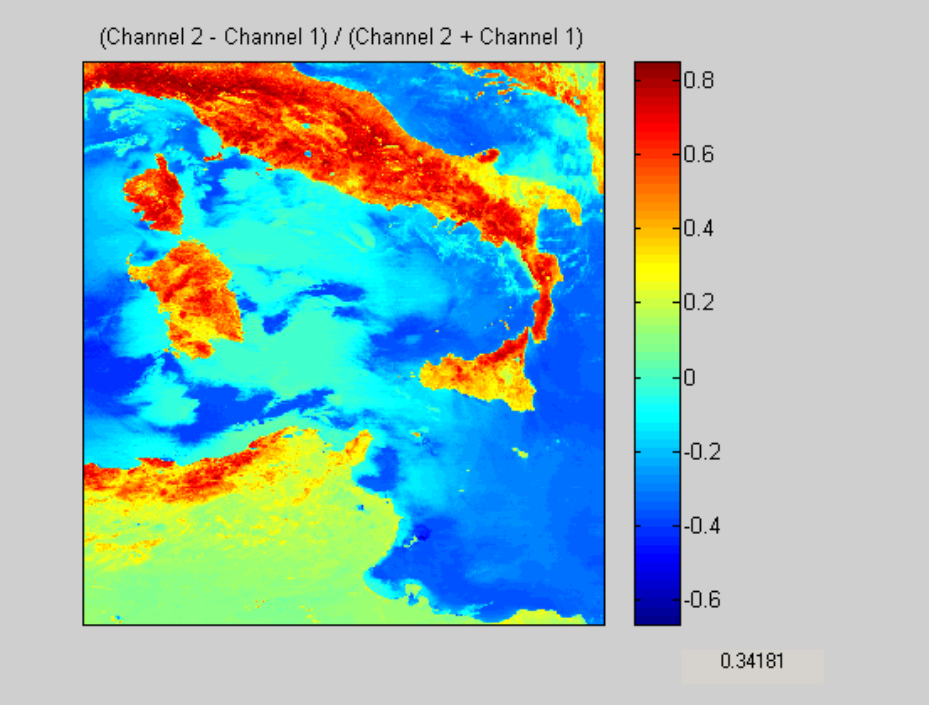

Figure 15.20: A pseudo image of normalized vegetation index [band 2 (0.86μm) – band 1 (0.65μm)] / [band 2 (0.86μm) – band 1 (0.65μm)] is displayed in Figure 15.20. Regions with some vegetation are clearly distinguished from those with little. Dry desert-like regions on the heel of Italy and in northern Africa show vegetation indices below 0.3; fertile valleys in northern Italy show indices above 0.8.

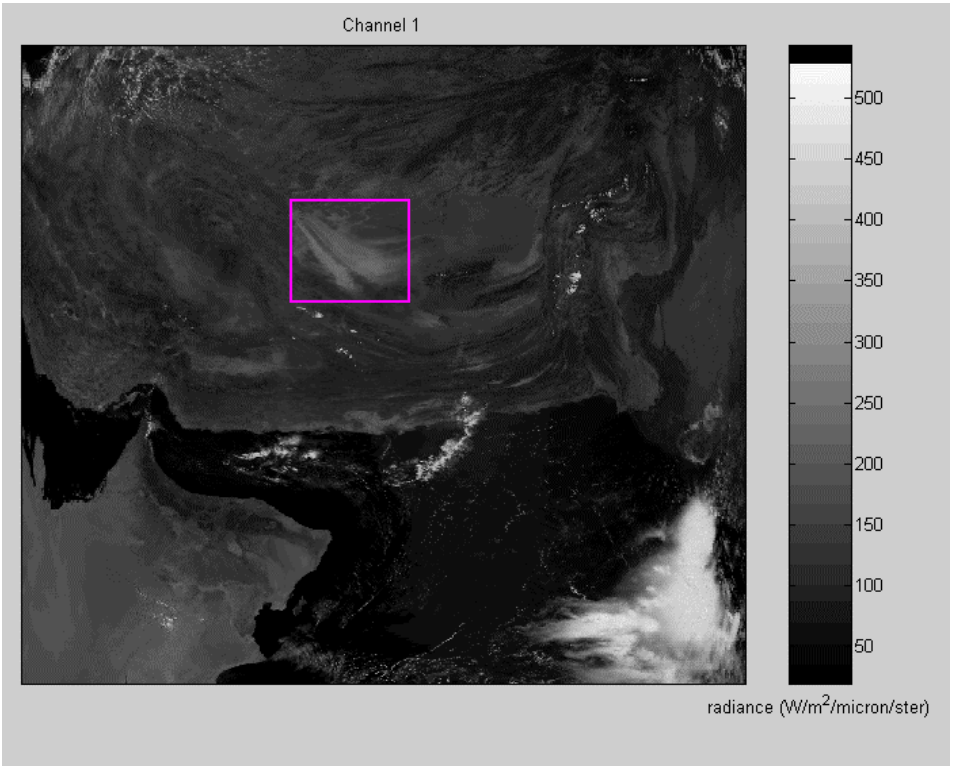

Figure 15.21: Dust storm in Iran on 11 June 2001 as seen by MODIS in the 0.65 um visible band 1.

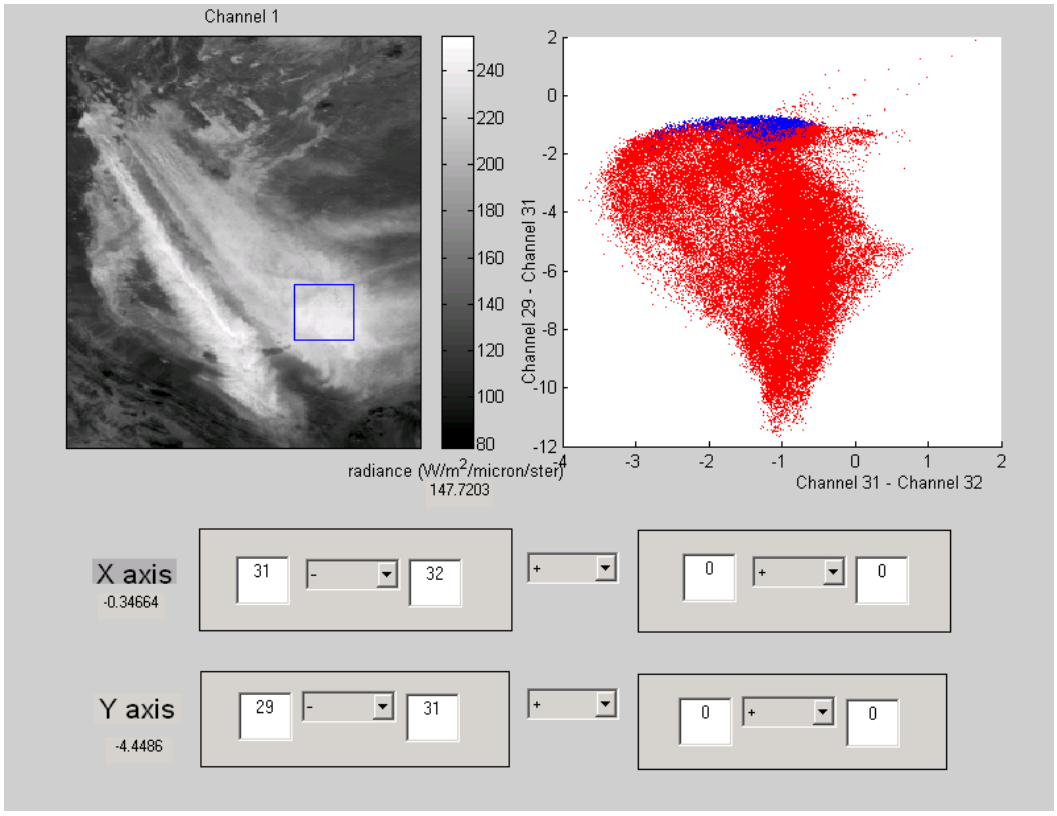

Figure 15.22: Scatter plot over dust storm of brightness temperature differences [band 29 (8.6μm) - band 31 (11μm)] on the y-axis and [band 31 (11μm) - band 32 (12μm)] on the x-axis. The dust storm produces brightness temperature differences between 0 and –2 C.

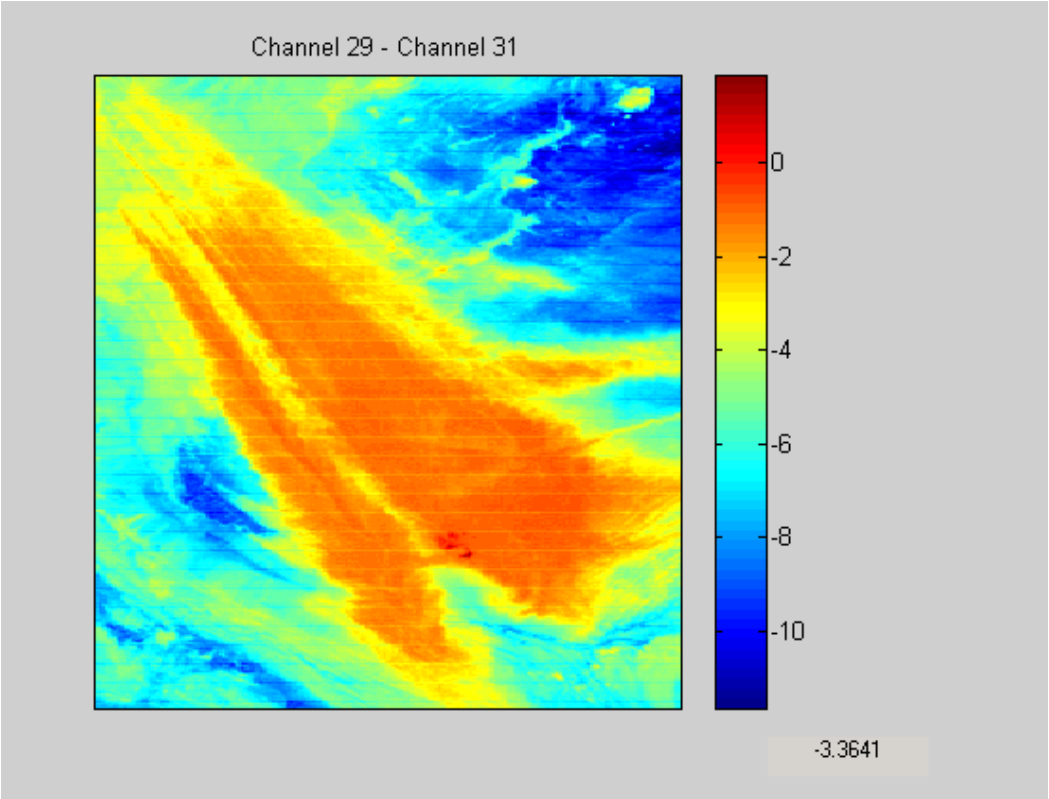

Figure 15.23: Pseudo channel plot over dust storm of [BT(8.6 um) – BT(11 um)]. Dust storm produces the least negative values in the scene.

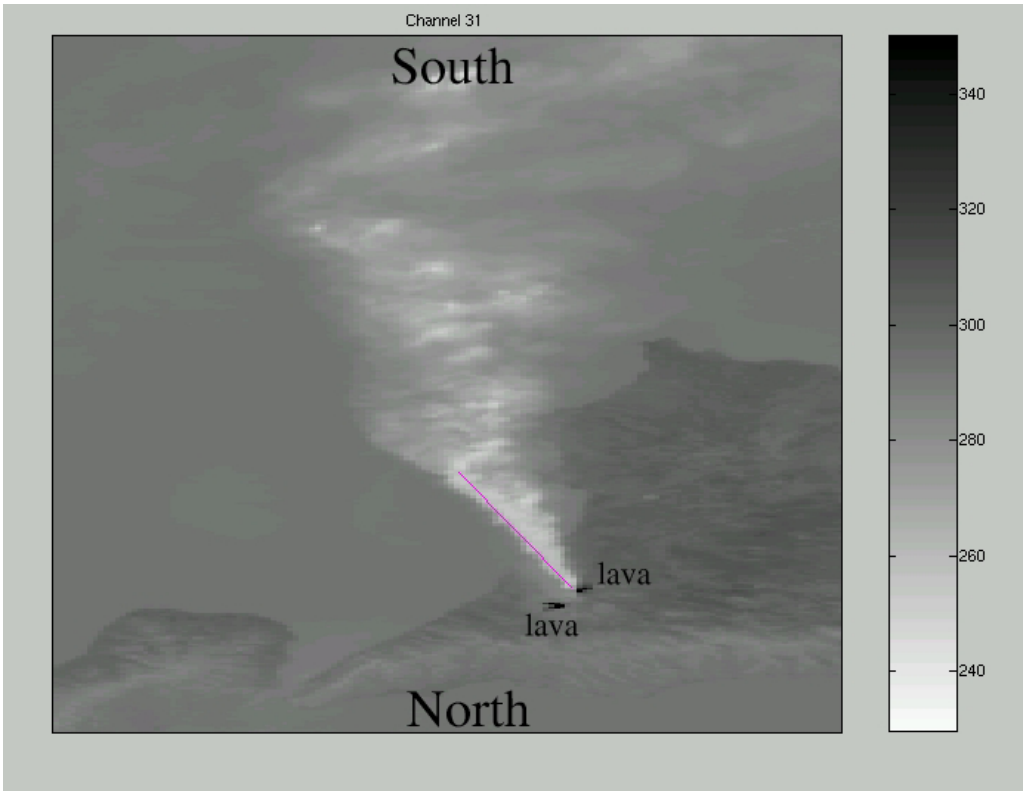

Figure 15.24: Mt Etna eruption on 28 October 2002 as seen by MODIS in the 11 um infrared window band 31.

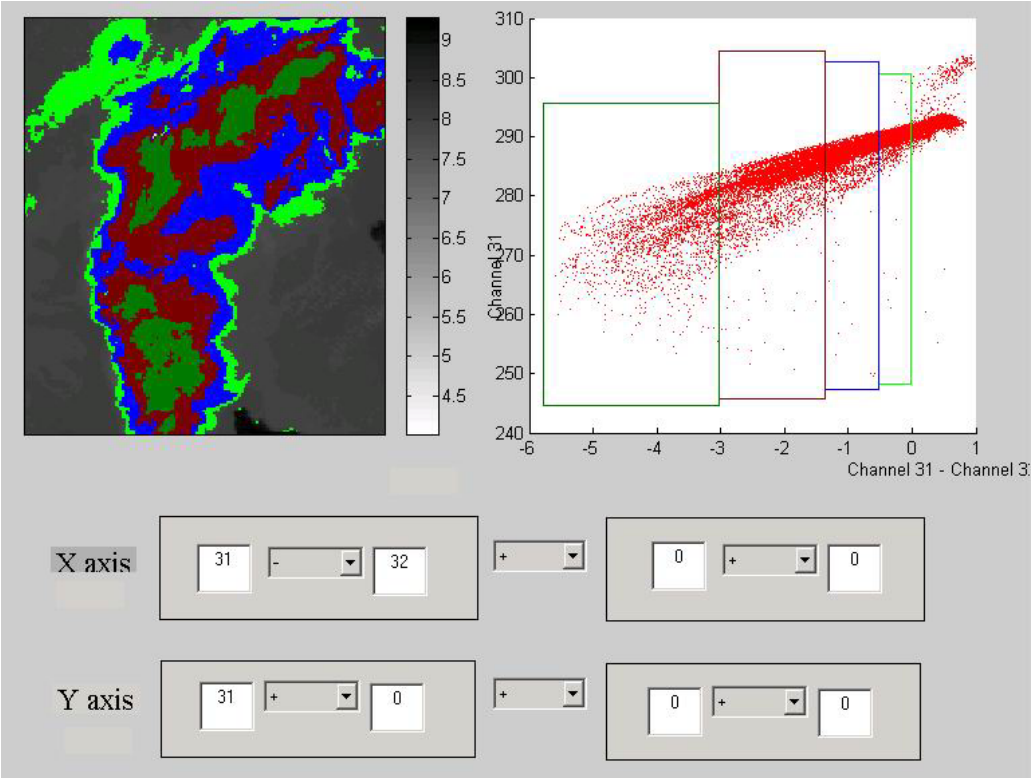

Figure 15.25: Scatter plot over Mt Etna eruption of [band 31 (11μm) - band 32 (12μm)] on the x-axis. The volcanic ash produces brightness temperature differences between 0 and –6 C.

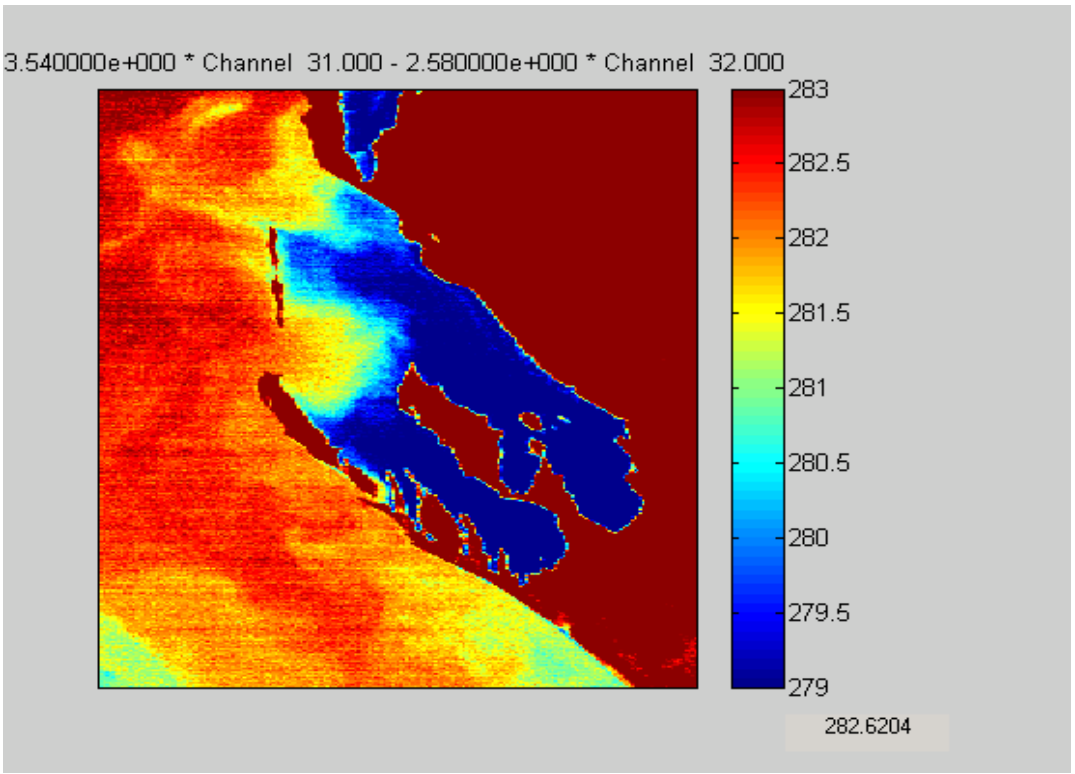

Figure 15.26: Image of sea surface temperature derived from the split window band 31 (11μm) and band 32 (12μm). Waters within Shark Bay are about 3 C cooler than the Leeuwin current waters along the WA coastline.

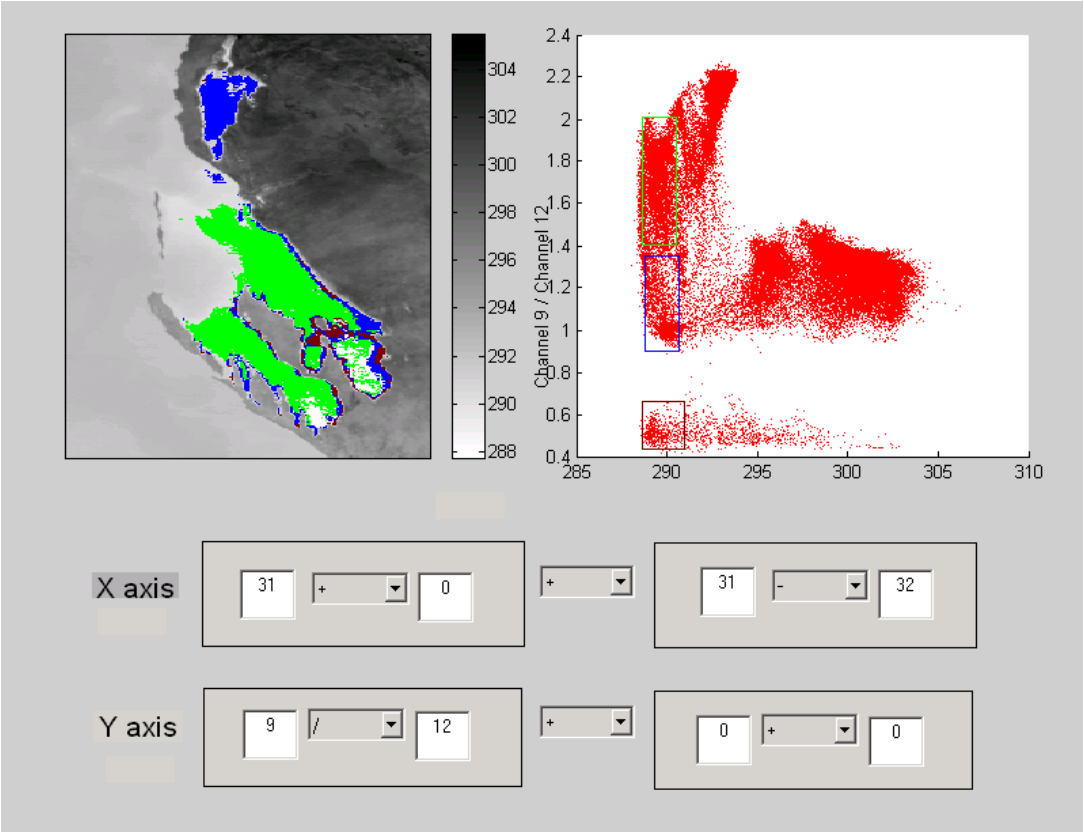

Figure 15.27: Scatter plot over Shark Bay of band 31 (11μm) on the x-axis and band 9 (0.44μm) / band 12 (0.57μm) on the y-axis. Low ratio values are an indication of chlorophyll concentrations.